Organic & Biomolecular Chemistry

ROYAL SOCIETY OF CHEMISTRY

PAPER

View Article Online
View Journal | View Issue

Cite this: *Org. Biomol. Chem.*, 2023, **21**, 3644

CPL-active water-soluble aromatic oligoamide foldamers†

Vincent Laffilé,‡[a] Kevin Moreno,‡[b] Eric Merlet,[a] Nathan McClenaghan,[b] Yann Ferrand*[a] and Céline Olivier*[b]

Received 24th March 2023,
Accepted 12th April 2023

DOI: 10.1039/d3ob00455d

rsc.li/obc

A series of enantiopure water-soluble quinoline-based foldamers were prepared and their optical and chiroptical properties in water were investigated. The new hexameric sequences incorporated either cationic or anionic water-solubilizing chains, and one of the oligomers was additionally functionalized by an electron donating moiety to further modulate the optoelectronic properties. A systematic study revealed strong electronic circular dichroism and circularly-polarized luminescence properties in water, with dissymmetry factors up to 2×10^{-2} in absorption and 5×10^{-3} in emission, regardless of the nature of the solubilizing chains and functions. This study therefore highlights new opportunities for the development of water-soluble and chiroptically-active artificial systems towards chirality-associated applications in aqueous or biological media.

Introduction

Chiral organic fluorophores that emit circularly polarized luminescence (CPL) have attracted considerable attention due to their potential application in the fields of 3D imaging, advanced security inks or device applications.[1] Furthermore, the circular polarization of emitted light may be used to study dynamic processes such as molecular chiral recognition.[2] However reports on effective CPL emission from chiral small organic molecules in water remain scarce,[3–7] limiting their potential application for biological purposes such as chiral analyte sensing or chiral bio-imaging.[8]

Asymmetry in organic compounds is primarily expressed as point chirality (*i.e.* asymmetric carbon), axial chirality (*i.e.* atropoisomerism) or helicity. The latter, although being the prominent expression of chirality at the macromolecular scale, involves intramolecular electronic interactions that may be sensitive to protic solvents. For this reason, water-soluble artificial helical structures represent challenging targets. In this regard, applying a bio-inspired strategy, Huc and co-workers developed several water-soluble helical architectures based on aromatic oligoamide[9–13] backbones. In addition to high helical stability in water, these oligomers have been shown to be highly tuneable. Unlike natural peptidic α-helices whose folding relies strongly on their side chains, aromatic oligoamide foldamers can be functionalized by various types of functional groups without any major impact on their helical stability. These modular molecular platforms were first used for their cell-penetrating capabilities and, as their nontoxicity were established, they were considered for biological applications.[9,10] Later, Huc *et al.* demonstrated that these artificial oligomers could serve as efficient DNA mimics paving the way to the design of novel inhibitors of protein–DNA interactions.[13] In parallel, we and others have reported on the CPL properties of related classes of quinoline oligomers in organic media.[14–18] Notably, functional oligoamide foldamers appended with different fluorophores were shown to display strong CPL emission at adjustable wavelengths.[14]

Herein, we report on the preparation of a series of enantiomerically pure water-soluble quinoline oligomers and the evaluation of their optical and chiroptical properties in water. For all sequences, quantitative helix handedness bias was achieved by introducing a camphanic acid moiety at the N terminus.[19] A systematic study was carried out on quinoline sequences bearing water-solubilizing chains including either cationic (*e.g.* ammonium or guanidinium) or anionic (phosphonate) functional groups. Cationic side-chains are known to assist cell-membrane permeation[10] whereas precisely positioned anionic side-chains can mimic DNA charge-surface.[13] Additionally, the substitution of a cationic side chain by an electron donating morpholine moiety was implemented to tune the emission wavelength of foldamers in polar solvents.

[a]*Institut de Chimie et Biologie des Membranes et Nanoobjets, UMR 5248 Université de Bordeaux, CNRS, IPB, 2 rue Escarpit, 33600 Pessac, France. E-mail: yann.ferrand@u-bordeaux.fr*

[b]*Institut des Sciences Moléculaires UMR 5255 Université de Bordeaux, CNRS, IPB, 351 cours de la Libération, 33405 Talence, France. E-mail: celine.olivier@u-bordeaux.fr*

†Electronic supplementary information (ESI) available: Spectroscopic and synthesis details. See DOI: https://doi.org/10.1039/d3ob00455d

‡These authors contributed equally to this work.

Results and discussion

Design and synthesis

First, it is worthy to note that unlike the preparation of functionalized organic solvent soluble aromatic oligoamides prepared by conventional multi-step synthesis requiring lengthy synthesis routes and purification, the preparation of water-soluble analogues can be achieved *via* straightforward solid-phase supported methods followed by HPLC purification. For this purpose, two new monomers Fmoc-$\mathbf{Q}^{\mathbf{Gua}}$-OH and Fmoc-$\mathbf{Q}^{\mathbf{Mor}}$-OH were prepared specifically. Fmoc-$\mathbf{Q}^{\mathbf{Gua}}$-OH was obtained from NO_2-$\mathbf{Q}^{\mathbf{Orn}}$-OMe using *N*,*N*′-bis(*tert*-butoxycarbonyl)-1*H*-pyrazole-1-carboxamidine to form the Boc protected guanidine side chain (Scheme S1†). Fmoc-$\mathbf{Q}^{\mathbf{Mor}}$-OH was prepared *via* the nucleophilic aromatic substitution of the bromine of NO_2-$\mathbf{Q}^{\mathbf{Br}}$-OMe by a morpholine residue (Scheme S2†). In both cases, after reduction of the nitro group and saponification of the methyl ester, the Fmoc group was introduced using 9-fluorenylmethyl chloroformate. Solid phase synthesis of sequences **1–4** (Fig. 1) were performed on low loading LL ProTide resin (0.17 mmol g^{-1}) using a Fmoc strategy (Schemes S4–S7†).[11] The first Fmoc-acid monomer was grafted using CsI and DIEA as a base in dry DMF. Fmoc-acid building blocks were activated *in situ* by generating the respective acid chlorides using an Appel reaction (PPh_3/trichloroacetonitrile) prior to coupling. One should note that *in situ* activation of Fmoc-$\mathbf{Q}^{\mathbf{Gua}}$-OH failed and was replaced by the pre-activation of the acid using Ghosez reagent prior to coupling (see the ESI†). Then, *S*- or *R*-camphanic chloride was reacted with the terminal amino group of sequences **1–4** to induce a *P* or *M* handedness, respectively. Finally, the oligomers were cleaved from the resin and the side chains deprotected under acidic conditions. After purification using semi-preparative reverse phase HPLC and salt exchange when necessary, sequence **1**, **3** and **4** were obtained in good overall purified yields (57–80%). Sequence **2** was obtained with a lower overall yield (7%) yet was sufficient for the study.

The foldamers prepared in this study are all hexameric quinoline-derived oligomers whose sequences are represented in Fig. 1. Sequence **1** is exclusively composed of $\mathbf{Q}^{\mathbf{Orn}}$ monomers whose water-solubilizing chain is a propyloxyammonium salt and as a result sequence **1** is a polycationic species. In the same way, sequence **2** is composed of $\mathbf{Q}^{\mathbf{Gua}}$ monomers only, in which the water-solubilizing chain is a propyloxyguanidinium salt, making it polycationic like **1**. On the contrary, **3** is a polyanionic sequence, composed of $\mathbf{Q}^{\mathbf{Pho}}$ monomers, bearing a methyloxyphosphonate chain. Finally, **4** is a hetero-oligomeric sequence composed of five $\mathbf{Q}^{\mathbf{Orn}}$ and one $\mathbf{Q}^{\mathbf{Mor}}$ monomers. The functionalized quinoline $\mathbf{Q}^{\mathbf{Mor}}$ was introduced at position 2 of the sequence, based on previous studies related to the positional isomerism of such functionalized oligoquinoline foldamers.[17] In addition to the four water-soluble hexameric sequences, Fig. 1 represents previously reported sequence **5**,[17] composed of $\mathbf{Q}^{\mathbf{Leu}}$ monomers, *i.e.* bearing isobutoxy chains that make it highly soluble in chlorinated solvents.

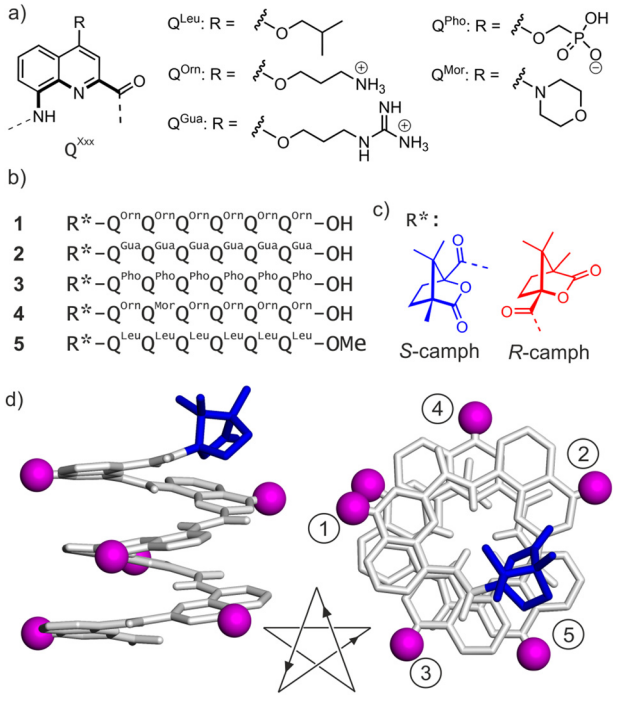

Fig. 1 (a) Structure of Q^{Xxx} (left) and the various side chains that were introduced in position 4 of the quinolone ring (right). The counter ions are trifluoroacetate and ammonium for cationic and anionic side chains, respectively. (b) Oligoamide sequences investigated in this study. (c) Formulae of the *R*- and *S*-camphanyl chiral inducers. (d) Energy minimized model (MMFFs) of the *P* helix of a canonical Q hexamer; the helix is shown in white stick representation, the purple spheres denote the position of the side chains, non-polar hydrogens are omitted for clarity.

Optical properties in water

The optical properties of the water-soluble sequences **1–4** were evaluated in pure water. The normalized UV-visible absorption and emission spectra are shown in Fig. 2 and the corres-

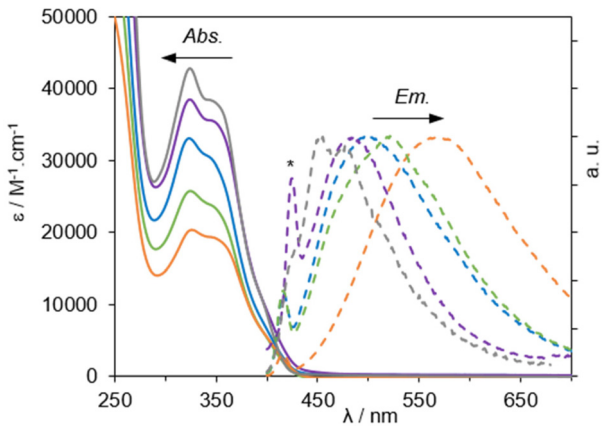

Fig. 2 Electronic absorption and normalised fluorescence emission spectra of the quinoline-derived hexamers **1** (blue), **2** (green), **3** (purple), **4** (orange) recorded in H_2O and **5** (grey) recorded in $CHCl_3$ ($C_{abs.}$ = 30 μM; λ_{exc} = 365 nm). * Raman scattered peak of water.[21]

Table 1 Optical and chiroptical properties of sequences **1**, **2**, **3** and **4**. Data corresponding to sequence **5** are reported for comparison according to ref. 17

	λ_{abs} [a] /nm	ε /M^{-1} cm^{-1}	$\lambda_{em.}$ [b]/nm	Φ_{lum} [c]/%	$\Delta\varepsilon$ [d]	g_{abs} [e]	g_{lum} [f]
1	323	33 000	502	0.10	(*P*) +82 (410), +108 (390)	(*P*) 1.8×10^{-2} (410), 1.0×10^{-2} (390)	(*P*) 3.4×10^{-3} (507)
	343	30 500			(*M*) −82 (410), −107 (390)	(*M*) -1.6×10^{-2} (410), -0.9×10^{-2} (390)	(*M*) -2.2×10^{-3} (507)
2	326	25 900	519	0.12	(*P*) +69 (408), +84 (390)	(*P*) 2.0×10^{-2} (410), 1.0×10^{-2} (390)	(*P*) 5.0×10^{-3} (507)
	348	23 700			(*M*) −68 (408), −83 (390)	(*M*) -2.0×10^{-2} (410), -1.0×10^{-2} (390)	(*M*) -4.0×10^{-3} (507)
3	324	38 500	484	0.01	(*P*) + 84 (408), + 105 (390)	(*P*) 2.1×10^{-2} (408), 1.0×10^{-2} (390)	(*P*) 5.3×10^{-3} (497)
	347	35 500			(*M*) −81 (408), −103 (390)	(*M*) -2.0×10^{-2} (408), -0.9×10^{-2} (390)	(*M*) -4.2×10^{-3} (497)
4	326	20 400	568	0.42	(*P*) +51 (410), +57 (393)	(*P*) 1.1×10^{-2} (410), 0.7×10^{-2} (393)	(*P*) 2.4×10^{-3} (558)
	347	19 300			(*M*) −49 (410), −55 (393)	(*M*) -1.1×10^{-2} (410), -0.7×10^{-2} (393)	(*M*) -1.3×10^{-3} (558)
5	325	42 900	452	6	(*P*) +88 (400), +100 (383)	(*P*) 1.1×10^{-2} (400), 0.6×10^{-2} (390)	(*P*) 1.3×10^{-2} (450)
[g]	350	38 200			(*M*) −76 (400), −86 (383)	(*M*) -1.0×10^{-2} (400), -0.5×10^{-2} (390)	(*M*) -1.1×10^{-2} (450)

[a] Maximum absorption wavelength in H_2O ($C = 3 \times 10^{-5}$ M). [b] Maximum emission wavelength in H_2O (λ_{exc} = 365 nm). [c] Fluorescence quantum yield. [d] Molar ellipticity. [e] Absorption dissymmetry factor and corresponding wavelength. [f] Luminescence dissymmetry factor and corresponding wavelength. [g] In $CHCl_3$ (data from ref. 17).

ponding values are regrouped in Table 1. The data corresponding to sequence **5** recorded in chloroform are indicated for comparison. All hexamers show comparable absorption profiles in solution. The spectra present intense absorption bands in the UV spectral region characteristic of the oligoquinoline backbone, which are primarily ascribed to $\pi \rightarrow \pi^*$ transitions, with some further contribution from $n \rightarrow \pi^*$ transitions. The main differences in absorption lie in the corresponding molar absorption coefficients that significantly vary depending on the nature of the solubilizing chains. Hexamer **3**, bearing negatively charged end-groups, exhibits the highest molar absorption coefficients of the series, ε_{max} = 38 500 and 35 500 M^{-1} cm^{-1}. These values are in the same range of those measured in chloroform for sequence **5** equipped with isobutoxy chains, ε = 42 000 M^{-1} cm^{-1} and 38 200 M^{-1} cm^{-1}. However, the hexamers bearing positively charged end-groups show a slightly lower absorption coefficient. Hexamer **1** bearing propyloxyammonium chains shows ε = 33 000 and 30 500 M^{-1} cm^{-1}, and upon replacing the ammonium groups by guanidinium end-groups as in sequence **2**, a net decrease of the molar absorption coefficient is observed, ε = 25 800 and 23 700 M^{-1} cm^{-1}. The morpholine-functionalized analogue **4** shows the lowest absorption intensity of the series with ε = 20 400 and 19 300 M^{-1} cm^{-1}. Overall, the molar absorption properties are thus generally preserved from an organic medium to an aqueous medium.

The emission properties of the water-soluble sequences were evaluated in pure dilute water solutions ($\sim 10^{-6}$ M) at room temperature. Overall, the fluorescence spectra show a broad unstructured band in the visible with red-shifted maximum emission compared to that of hexamer **5** recorded in chloroform (λ_{em} = 452 nm). Sequences **1** and **2** show maximum emission at λ_{em} = 502 nm and 519 nm, respectively, which represent significant red-shifts of 50 nm and 67 nm compared to **5** in $CHCl_3$. Hexamer **3**, bearing negatively charged end-groups, exhibits a smaller red-shift of 32 nm corresponding to an emission maximum at λ_{em} = 484 nm. In general, the photoluminescence of discrete molecules in solution originates from the relaxation of the system from its photoexcited state to the ground-state, and this phenomenon is related to the HOMO–LUMO energy gap of the molecule. The red-shifting of the emission maxima observed in water compared to organic solvent therefore corresponds to a reduction of the HOMO–LUMO gap presumably due to interactions of the molecules with the highly polar water solvent and which also allows rapid non-radiative decay of the excited state by vibrational relaxation due to the presence of vicinal O–H oscillators.

As expected, hexamer **4** bearing ammonium end-groups plus an additional morpholine functional group, presents further increased red-shifting of the emission, with λ_{em} = 568 nm, and consequently a large Stokes shift of 221 nm ($\Delta\nu$ = 11 213 cm^{-1}). This appealing property of **4** might be advantageous in the context of fluorescence imaging applications, since the wide gap between the excitation and emission maxima diminishes self-absorption phenomena.

The fluorescence quantum yields evaluated for the non-functionalized hydrophilic hexameric sequences **1–3** in water range from 0.01% to 0.12%. These values are lower than that of sequence **5** recorded in chloroform (Φ_{lum} = 6%) as one could expect from the enhanced non-radiative deactivation processes occurring in polar protic solvents such as water.[20] Nonetheless, thanks to the presence of the morpholine group acting as electron donating unit, sequence **4** yields slightly higher fluorescence quantum yield of Φ_{lum} = 0.42%, thus showing that modulation of the emission properties of quinoline-based oligomers is also possible in water.

Chiroptical properties in water

The chiroptical properties of the two *P* and *M* enantiomers of each water-soluble sequence were evaluated in pure water using electronic circular dichroism (ECD) and circularly polarized luminescence (CPL). The spectra are shown in Fig. 3 and the corresponding values are regrouped in Table 1. Regardless of the nature of the solubilizing chains, intense ECD signals are typically observed for the different water-soluble oligoamides confirming the efficient folding of these oligomers as supramolecular helices even in aqueous medium. Similar to

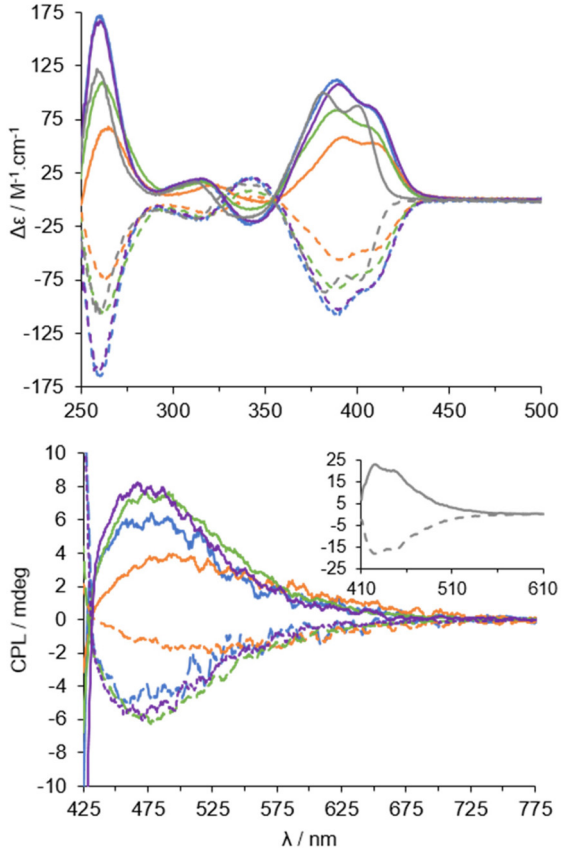

Fig. 3 ECD (top) and CPL (bottom) spectra of the quinoline-derived hexamers *P*-**1** (blue, solid), *M*-**1** (blue, dashed), *P*-**2** (green, solid), *M*-**2** (green, dashed), *P*-**3** (purple, solid), *M*-**3** (purple, dashed), *P*-**4** (orange, solid), *M*-**4** (orange, dashed) recorded in pure water and *P*-**5** (grey, solid), *M*-**5** (grey, dashed) recorded in $CHCl_3$ (C = 30 μM; λ_{exc} = 365 nm).

what was observed with sequence **5** in chloroform, the ECD spectra of the water-soluble hexamers show multiple Cotton effects corresponding to their UV-visible absorption region. Notably, two intense absorption bands are observed around 410 and 390 nm that are characteristic of quinoline oligomers. As in organic solvents, the *P* enantiomers yield a positive Cotton effect at low energy, while *M* enantiomers yield a negative Cotton band. Two bands of weaker intensities and with sign inversions are observed between 280 and 370 nm. Finally, an intense band is systematically observed at 260 nm, which is positive for the *P* enantiomers and negative for *M* enantiomers.

Hexamers **1** and **3**, bearing positively-charged propyloxyammonium chains and negatively-charged methyloxyphosphonate chains, respectively, present quasi-superimposable ECD spectra. This tends to indicate that the nature of the solubilizing end-groups (positively- or negatively-charged) has no (or little) impact on the chirality of the ground-state electronic transitions. In terms of intensity of the ECD response, those of sequences **2** and **4** are slightly weaker than that of sequences **1** and **3**. The maximum molar circular dichroism values range from $\Delta\varepsilon_{max}$ = 108 M^{-1} cm^{-1} for *P*-**1** to 84 M^{-1} cm^{-1} and 57 M^{-1} cm^{-1}, for *P*-**2** and *P*-**4**, respectively. This, in the case of **4**, suggests an electronic perturbation occurring within the functionalized oligomer in its ground state, similar to previously reported functionalized quinoline hexamers.[17] To quantitatively assess the magnitude of the ECD, the dimensionless Kuhn's anisotropy factor in the ground state, *i.e.* absorption dissymmetry factor, defined as $g_{abs} = \Delta\varepsilon/\varepsilon$, was considered. Thus, the water-soluble hexameric sequences **2** and **3** show g_{abs} up to 2×10^{-2}, which is slightly higher than sequence **5** in chloroform. Such g_{abs} values are one order of magnitude higher in comparison to the *C*2-symmetric water-soluble binaphthyl fluorophores reported by Imai,[4] and it is also higher than that recently reported for a chromophoric π-extended aza[7]helicenium in an aqueous medium.[7]

The chiral emission properties of the new hexamer series were further assessed in water. Irrespective of the nature of the solubilizing chains, and similar to the chiral absorption properties, a CPL response was systematically observed for the different oligomers in aqueous solution. The sign of the CPL signals was the same as the low-energy ECD signals, *i.e.* positive for the *P* enantiomers and negative for the *M* enantiomers. Hence the local chirality of the corresponding electronic transitions is conserved in the ground- and excited-states. The circularly polarized emission range of the water-soluble oligomers corresponds to that of the total unpolarised photoluminescence (PL) in water. The Kuhn's anisotropy factors in the photoexcited state, *i.e.* luminescence dissymmetry factors g_{lum}, were therefore calculated considering the CPL intensity at maximum PL. Overall, the water-soluble sequences exhibit significant CPL activity, with g_{lum} values ranging from 1.3×10^{-3} (*M*-**4**) to 5.3×10^{-3} (*P*-**2**) at maximum PL, which represents remarkable chiral emission for small organic molecules.[22,23]

Sequences **1**, **2** and **3** display comparable CPL intensities with $g_{lum} = 3.4 \times 10^{-3}$ to 5.3×10^{-3} for the *P* enantiomers, indicating that the nature of the water-solubilizing chains has only poor influence on the chiral emission properties. The three water-soluble hexameric sequences devoid of additional functional group therefore show slightly lower dissymmetry in emission than sequence **5** in chloroform ($g_{lum} = 1.1 \times 10^{-2}$ for *P*-**5**).

Nonetheless, the g_{lum} values reported herein are in the same range of previously reported aza[7]helicenium in H_2O/MeOH solvent mixture ($g_{lum} = 6 \times 10^{-3}$)[7] and they are significantly higher than that of functionalized binaphthyl fluorophores in water and in MeOH ($g_{lum} = 4 \times 10^{-4}$).[4] As for the fluorescence emission, the electronically enriched sequence **4** exhibits red-shifted CPL signal compared to the non-functionalized water-soluble sequences, yielding CPL emission at λ = 558 nm with an associated $g_{lum} = 2.4 \times 10^{-3}$ for *P*-**4**. The slightly lower CPL intensity observed for the functionalized sequence **4** compared to the hexamers without additional substituents is consistent with previous observations in organic solvent and stems from the perturbation of the excited states related to the presence of the achiral fluorophore on the chiral oligomeric helices.[14,17]

A correlation between the absorption and emission dissymmetry factors (g_{abs} and g_{lum}) was established by Mori *et al.* con-

sidering several categories of chiral small organic molecules.[23] Although the supramolecular helices reported in the present study do not fall into the categories described in this review article, their characteristics are in line with other molecules of helical chirality (*i.e.* helicenes and helicenoids). The general trend is $g_{lum} < g_{abs}$, to a greater or lesser extent related to the conformational flexibility of the molecules in their excited state. In particular the authors consider the g_{lum}/g_{abs} ratio to quantify the difference in asymmetry between the chiroptical properties of absorption and emission. In the present study, this ratio falls in the range of 0.25 (sequence **1**) to 0.5 (sequence **3**) which, as expected from these dynamic supramolecular architectures, further testifies to the importance of processes of vibrational relaxation on the excited-state through both conformational flexibility and interaction with the polar solvent.

Conclusions

In summary, a series of eight water-soluble quinoline-based oligoamide foldamers was readily prepared through solid-phase supported synthesis for assessment of their optical and chiroptical properties in water. The hexameric sequences were equipped with different types of solubilizing chains, either cationic or anionic, and derivatized with a camphanyl chiral inducer for complete handedness bias induction, leading to *P*- and *M*-helices selectively. In addition, one of the new sequences incorporated a morpholine functional group to study its influence on the optoelectronic properties of the foldamer in water. Whatever the nature of the polar end-group present on the solubilizing chains (*i.e.* ammonium, guanidinium or phosphonate), the helical folding of the oligoamide architectures was confirmed by spectroscopic characterizations. The systematic study carried out in pure water revealed strong chiroptical properties, as proved by ECD and CPL spectroscopies, thus validating our approach of using oligoquinoline foldamers to generate circularly polarized emission in water.

Through this study we therefore demonstrate that oligoquinoline foldamers represent a highly modular molecular platform to observe chiroptical activity, both in absorption and emission, in a variety of solvents including pure water. This represents a new step forward for (supra)molecular chiral emitters towards bio-related applications such as chiroptical bioimaging.

Experimental section

General procedures for oligomer SPS

Resin grafting. On *LL* ProTide resin (0.17 mmol g^{-1}), the first Fmoc(Q^R)CO_2H monomer (3 equiv.) was grafted using CsI (5 equiv.) and DIEA (6 equiv.) in dry DMF. The reaction mixture was shaken vigorously overnight. After reaction, the resin was filtered and washed three times with DMF and three times with dichloromethane.

Fmoc deprotection. Grafted resin was washed twice with DMF, suspended in a 20% piperidine in DMF solution (4 mL) and slowly stirred for 3 minutes. The resin was then filtered, washed twice with DMF and resuspended in a 20% piperidine in DMF solution and stirred for 7 minutes. The resin was then filtered and washed three times with DMF and three times with dry THF.

***In situ* coupling procedure (Q^{orn}, Q^{Pho}, Q^{Mor}).** The resin was suspended in dry THF and collidine (9 equiv.) was added. A solution of Fmoc(Q^X)CO_2H monomer (3 equiv.), PPh_3 (8 equiv.) and TCAN (9 equiv.) in dry $CHCl_3$ was added to the resin. The reaction was assisted by microwave irradiation (25 W, 50 °C) for 15 minutes and repeated once. After reaction, the resin was filtered and washed with dry THF and DMF.

Acid chloride coupling procedure (Q^{Gua}). The resin was suspended in dry THF and DIEA (6 equiv.) was added. Fmoc(Q^{Gua})COCl monomer (3 equiv., Scheme S3†) was dissolved in dry THF and added to the resin. The reaction was assisted by microwave irradiation (50 W, 50 °C) for 15 minutes and repeated once. The resin was then filtered and rinsed with dry THF and DMF.

Resin cleavage. The resin was washed three times with DMF and three times with dichloromethane and was suspended in a solution of TFA/TIPS/H_2O 95 : 2.5 : 2.5 (v/v/v). The mixture was vigorously stirred for 4 hours. The resin was filtered and the filtrate was evaporated under reduced pressure. The residual solid was suspended in Et_2O and centrifuged at 4 °C for 5 minutes. Et_2O was removed and the yellow solid was dried under vacuum and then freeze-dried.

Preparative HPLC purification. For sequences containing Q^{Orn} and Q^{Gua} monomers. Crude compounds were purified using solvents A and B. The following gradient was used: (0 min): 95% A, 5% B then (2 min): 95% A, 5% B then (22 min): 0% A, 100% B then (27 min): 0% A, 100% B. Collected fractions were analyzed by analytic HPLC and the relevant ones were combined and freeze-dried twice to remove the excess of TFA.

For sequences containing Q^{Pho} monomers. Crude compounds were purified using solvents A′ and B′. The following gradient was used: (0 min): 95% A, 5% B then (2 min): 95% A, 5% B then (22 min): 0% A, 100% B then (27 min): 0% A, 100% B. Collected fractions were analyzed by analytic HPLC and the relevant ones were combined and freeze-dried twice to remove the excess of triethylammonium acetate.

Conflicts of interest

There are no conflicts to declare.

Acknowledgements

The University of Bordeaux and IdEx Bordeaux are greatly acknowledged for financial support (PhD grant to K. M).

V. L thanks ANR for PhD grant (ANR POLYnESI grant no. ANR-18-CE29-0013).

References

1 Y. Deng, M. Wang, Y. Zhuang, S. Liu, W. Huang and Q. Zhao, Circularly Polarized Luminescence from Organic Micro-/Nano-Structures, *Light: Sci. Appl.*, 2021, **10**, 76.
2 S. C. J. Meskers, Circular Polarization of Luminescence as a Tool to Study Molecular Dynamical Processes, *ChemPhotoChem*, 2022, **6**, e2002100154.
3 S. Pascal, C. Besnard, F. Zinna, L. Di Bari, B. Le Guennic, D. Jacquemin and J. Lacour, Zwitterionic [4]helicene: a water-soluble and reversible pH-triggered ECD/CPL chiroptical switch in the UV and red spectral regions, *Org. Biomol. Chem.*, 2016, **14**, 4590–4594.
4 T. Kitatobe, Y. Mimura, S. Tsujimoto, N. Tajima, M. Fujiki and Y. Imai, Circularly polarized luminescence from open- and closed-style axially chiral amphipathic binaphthyl fluorophores in water, *Tetrahedron*, 2017, **73**, 6856–6862.
5 T. He, C. Ren, Y. Luo, Q. Wang, J. Li, X. Lin, C. Ye, W. Hu and J. Zhang, Water-soluble chiral tetrazine derivatives: towards the application of circularly polarized luminescence from upper-excited states to photodynamic therapy, *Chem. Sci.*, 2019, **10**, 4163–4168.
6 Y. Mimura, Y. Motomura, M. Kitamatsu and Y. Imai, Sign inversion of excimer circularly polarized luminescence in water-soluble bipyrenyl oligopeptides through an odd-even effect, *Tetrahedron Lett.*, 2020, **61**, 152238–154168.
7 C. Olivier, N. Nagatomo, T. Mori, N. McClenaghan, G. Jonusauskas, B. Kauffmann, Y. Kuwahara, M. Takafuji, H. Ihara and Y. Ferrand, A π-extended phenanthrene-fused aza[7]helicenium as novel chiroptically-active architecture in organic and aqueous media, *Org. Chem. Front.*, 2023, **10**, 752–758.
8 K. Staszak, K. Wieszczycka, V. Marturano and B. Tylkowski, Lanthanides Complexes – Chiral Sensing of Biomolecules, *Coord. Chem. Rev.*, 2019, **397**, 76–90.
9 E. R. Gillies, F. Deiss, C. Staedel, J.–M. Schmitter and I. Huc, Development and Biological Assessment of Fully Water-Soluble Helical Aromatic Amide Foldamers, *Angew. Chem., Int. Ed.*, 2007, **46**, 4081–4084.
10 J. Iriondo, K. Laxmi-Reddy, B. Bouguerne, C. Staedel and I. Huc, Cellular Internalization of Water-Soluble Helical Aromatic Amide Foldamers, *ChemBioChem*, 2010, **11**, 1679–1685.
11 B. Baptiste, C. Douat-Casassus, K. Laxmi-Reddy, F. Godde and I. Huc, Solid Phase Synthesis of Aromatic Oligoamides: Application to Helical Water-Soluble Foldamers, *J. Org. Chem.*, 2010, **75**, 7175–7185.
12 S. J. Dawson, A. Meszaros, L. Petho, C. Colombo, M. Csékei, A. Kotschy and I. Huc, Controlling Helix Handedness in Water-Soluble Quinoline Oligoamide Foldamers, *Eur. J. Org. Chem.*, 2014, 4265–4275.
13 K. Ziach, C. Chollet, V. Parissi, P. Prabhakaran, M. Marchivie, V. Corvaglia, P. P. Bose, K. Laxmi-Reddy, F. Godde, J.-M. Schmitter, S. Chaignepain, P. Pourquier and I. Huc, Single Helically Folded Aromatic Oligoamides that Mimic the Charge Surface of Double-Stranded B-DNA, *Nat. Chem.*, 2018, **10**, 511–518.
14 E. Merlet, K. Moreno, A. Tron, N. McClenaghan, B. Kauffmann, Y. Ferrand and C. Olivier, Aromatic Oligoamide Foldamers as Versatile Scaffolds for Induced Circularly Polarized Luminescence at Adjustable Wavelengths, *Chem. Commun.*, 2019, **55**, 9825–9828.
15 D. Zheng, L. Zheng, C. Yu, Y. Zhan, Y. Wang and H. Jiang, Significant Enhancement of Circularly Polarized Luminescence Dissymmetry Factors in Quinoline Oligoamide Foldamers with Absolute Helicity, *Org. Lett.*, 2019, **21**, 2555–2559.
16 D. Zheng, C. Yu, L. Zheng, Y. Zhan and H. Jiang, Absolute Control of Helicity at the C-termini in Quinoline Oligoamide Foldamers by Chiral Oxazolylaniline Moieties, *Chin. Chem. Lett.*, 2020, **31**, 673–676.
17 K. Moreno, E. Merlet, N. McClenaghan, T. Buffeteau, Y. Ferrand and C. Olivier, Influence of Positional Isomerism on the Chiroptical Properties of Functional Aromatic Oligoamide Foldamers, *ChemPlusChem*, 2021, **86**, 496–503.
18 D. Zheng, S. Guo, L. Zheng, Q. Xu, Y. Wang and H. Jiang, Red Circularly Polarized Luminescence from Intramolecular Excimers Restricted by Chiral Aromatic Foldamers, *Chem. Commun.*, 2021, **57**, 12016–12019.
19 A. M. Kendhale, L. Poniman, Z. Dong, K. Laxmi-Reddy, B. Kauffmann, Y. Ferrand and I. Huc, Absolute Control of Helical Handedness in Quinoline Oligoamides, *J. Org. Chem.*, 2011, **76**, 195–200.
20 J. Maillard, K. Klehs, C. Rumble, E. Vauthey, M. Heilemann and A. Fürstenberg, Universal Quenching of Common Fluorescent Probes by Water and Alcohols, *Chem. Sci.*, 2021, **12**, 1352–1362.
21 A. J. Lawaetz and C. A. Stedmon, Fluorescence Intensity Calibration Using the Raman Scatter Peak of Water, *Appl. Spectrosc.*, 2009, **63**, 936–940.
22 E. M. Sanchez-Carnerero, A. R. Agarrabeitia, F. Moreno, B. L. Maroto, G. Muller, M. J. Ortiz and S. de la Moya, Circularly Polarized Luminescence from Simple Organic Molecules, *Chem. – Eur. J.*, 2015, **21**, 13488.
23 H. Tanaka, Y. Inoue and T. Mori, Circularly Polarized Luminescence and Circular Dichroisms in Small Organic Molecules: Correlation between Excitation and Emission Dissymmetry Factors, *ChemPhotoChem*, 2018, **2**, 386.